Hindawi Publishing Corporation
International Journal of Photoenergy
Volume 2015, Article ID 414851, 8 pages
http://dx.doi.org/10.1155/2015/414851

Research Article

Synergetic Enhancement of Device Efficiency in Poly(3-hexylthiophene-2,5-diyl)/[6,6]-phenyl C_{61} Butyric Acid Methyl Ester Bulk Heterojunction Solar Cells by Glycerol Addition in the Active Layer

Bobins Augustine and Tapio Fabritius

University of Oulu, Department of Electrical Engineering, Optoelectronics and Measurement Laboratory, Erkki Koiso-Kanttilan Katu 3, 90570 Oulu, Finland

Correspondence should be addressed to Bobins Augustine; baugusti@ee.oulu.fi

Received 12 August 2014; Revised 2 March 2015; Accepted 14 March 2015

Academic Editor: Věra Cimrová

Poly(3-hexylthiophene-2,5-diyl)(P3HT):[6,6]-phenyl-C61-butyric acid methyl ester ($PC_{60}BM$) is the widely used active layer for the bulk heterojunction solar cells. Annealing is essential for P3HT:$PC_{60}BM$ active layer, since it facilitates the creation of better network for the transfer of the charge carriers. However, the $PC_{60}BM$ in the active layer can crystallize excessively during annealing treatments and disrupt the favorable morphology by forming crystallites in micrometer ranges, thus reducing device efficiency. In this paper we used glycerol as an additive in the active layer. Due to high boiling point of glycerol, it makes slow drying of the active layer possible during the annealing. It thus gives enough time to both electron donor (P3HT) and electron acceptor ($PC_{60}BM$) components of the active layer to self-organize and also restrict the crystal overgrowth of $PC_{60}BM$. Further, the glycerol additive makes the active layer smoother, which may also improve adhesion between the electrode and the active layer. The devices with the pristine active layer showed a power conversion efficiency (PCE) of about 2.1% and, with the addition of 30 vol% of glycerol in the active layer, the PCE value increased to 3%.

1. Introduction

The growing demand of sustainable sources of energy and the increasing interest in organic electronics have triggered huge attention to photovoltaic (PV) devices based on organic molecules (OPV). These types of solar cells which are potentially cheap and easy to process [1–4] offer new application opportunities and thereby are likely to enlarge the global usage of solar energy. One of the most studied active layers in the bulk heterojunction solar cell is poly(3-hexylthiophene-2,5-diyl) (P3HT) blended with [6, 6]-phenyl-C61-butyric acid methyl ester ($PC_{60}BM$).

The P3HT acts as the electron donor (D) and $PC_{60}BM$ acts as the electron acceptor (A) component of the active layer. The absorption of photon in organic semiconductors results in the formation of strongly bound electron-hole pairs called excitons. In order to obtain charge separation, it has to diffuse to the dissociation sites. The interface between P3HT (donor) and $PC_{60}BM$ (acceptor) provides the dissociation site for the generated excitons where the energy difference in the electron affinities and the ionization potentials of the two donor and acceptor materials is large enough to overcome the exciton binding energy. After breaking of exciton binding energy, the charges are separated as free electron and holes which travel through the acceptor and donor phase, respectively, to the electrodes of the device [5]. The performance of these polymer solar cells is strongly dependent on the morphology of the constituting active layer. The D-A material morphology is very sensitive to heating processes. Annealing treatment is essential for the P3HT:$PC_{60}BM$ blend since it will create better networks between donor and acceptor molecules and also help to increase the P3HT crystallinity [6, 7]. However, during annealing treatments, the segregation of $PC_{60}BM$ into microsized crystallites can occur, which in turn

reduces the area of the donor-acceptor interface and destroys the continuous carrier path along which charges are transported to electrodes [8]. This degrades the device efficiency. It was reported that [9], for obtaining higher performing devices, the donor and acceptor materials in the active layer should be in the form of nanoscale bicontinuous networks of crystallites and there should be no excessive micrometer scale crystallizations.

Recently, several methods were adopted by researchers to limit the drawback of excessive crystallization, but most of the methods involve quite expensive additives and complicated chemical modifications [10–12]. In this paper we discovered the use of a very inexpensive and simple additive, resulting in the enhancement of the morphology of the blend and hence the device efficiency.

2. Experimental Section

2.1. Materials and Device Fabrication. The glass substrates with patterned indium tin oxide (ITO) stripes were supplied by Thin Film Devices Inc. (TFD). The square glass substrates with a dimension of 6.25 cm^2 were covered in the middle part with a 1.3 cm wide ITO stripe. The ITO thickness was 150 nm and had 20 ohm/sq sheet resistance. The substrates were first cleaned with acetone followed by isopropanol and methanol. Then they were plasma treated by Plasma PREEN II-862 asher (60 Watts, flow rate 4-5SCFM), for 1 minute.

Further, the hole transporting layer, poly(3,4-ethylenedioxythiophene)-poly(styrene sulfonate), PH500 was spin-coated at 6700 RPM for 1 minute and subsequently dried under a vacuum at 120°C for 1 hour. PH500 was supplied by H. C. Stark. Poly(3-hexylthiophene-2,5-diyl)(P3HT) was supplied by Sigma-Aldrich and [6, 6]-phenyl-C61-butyric acid methyl ester ($PC_{60}BM$) was supplied by NanoC.

The P3HT:$PC_{60}BM$ active layer blend was formed by making the solution in the ratio 1 : 0.8 with a concentration of 30 mg/mL, dissolved in 1,2-dichlorobenzene (DCB). Then solutions were made with the glycerol additive in the active layer blend with concentrations ranging from 0 vol% to 70 vol% with 10% intervals. The solutions were stirred at 55°C overnight. The active layer blends containing glycerol additive with the mentioned concentrations were then spin-coated at 450 RPM for 2 minutes inside a glove box. After drying these samples for 1 hour at room temperature in the nitrogen filled glove box, they were annealed at 150°C for 30 minutes. Then 0.6 nm of lithium fluoride (LiF) and 120 nm of aluminium (Al) layers were deposited, respectively, as electrodes by vacuum vapor deposition at 10^{-7} Torr. The finished solar cell had an active area of 15 mm^2.

2.2. Device Characterization. The unencapsulated solar cells were tested under ambient conditions using an Air Mass 1.5, class AAA solar simulator (Oriel Inc.) as the light source, and the light intensity was calibrated to be 100 mW/cm^2 by using a National Renewable Energy Laboratory calibrated crystalline Silicon cell as the reference. The measurements were done inside a nitrogen-filled glove box. The parameters, open circuit voltage (V_{oc}), short circuit current (I_{sc}), fill factor (FF), and power conversion efficiency (PCE) were obtained from corresponding current density- (J-) voltage (V) curves. For average measurements, 15 solar cells with an active area of 15 mm^2 each were taken for each device with varying additive concentrations.

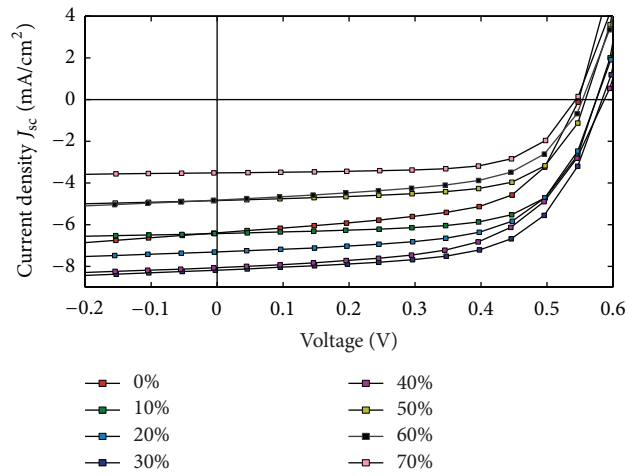

FIGURE 1: J-V characteristics of organic solar cells with the active layer containing a glycerol additive of varying concentrations.

For atomic force microscopy (AFM), the system Veeco Dimension 3100 was used and the measurements were done using the tapping mode. A silicon tip with radius around 10 nm was used as a probe on the surface. The projected image area of the AFM was 25 μm^2. For optical microscope investigation, a Nikon universal design microscope (UDM) ECLIPSE LV100DA-U was utilized.

3. Results and Discussion

3.1. Effect on Photovoltaic Parameters of the Device with Glycerol Addition in the Active Layer. The active layer was a blend of P3HT and $PC_{60}BM$ which was dissolved in 1,2-dichlorobenzene (DCB). Glycerol, which has a higher boiling point of 290°C [13], was used as an additive in the active layer to slow down the rapid evaporation of the solvent in the layer during annealing. The spin-coated active layers, with glycerol additives of varying concentrations, were dried at room temperature inside glove box for 1 hour and subsequently annealed for 30 minutes at 150°C [14]. Figure 1 shows the current density-voltage (J-V) characteristics of the best performing devices.

From the J-V curves in Figure 1, it is evident that the performances were good for devices containing 30 vol% glycerol additive in the active layer. The pristine devices with 0 vol% glycerol additive showed an open circuit voltage (V_{oc}) of 0.55 V, short circuit current density (J_{sc}) of 6.38 mA/cm^2, fill factor (FF) of 59.4%, and power conversion efficiency (PCE) of 2.1%. But with the addition of 30 vol% glycerol, the V_{oc} increased to 0.586 V, J_{sc} increased to 8.19 mA/cm^2, FF increased to 62%, and the PCE was enhanced to 3%. There was a sharp increase of 42% in PCE values with 30 vol% glycerol addition. The current density values were enhanced

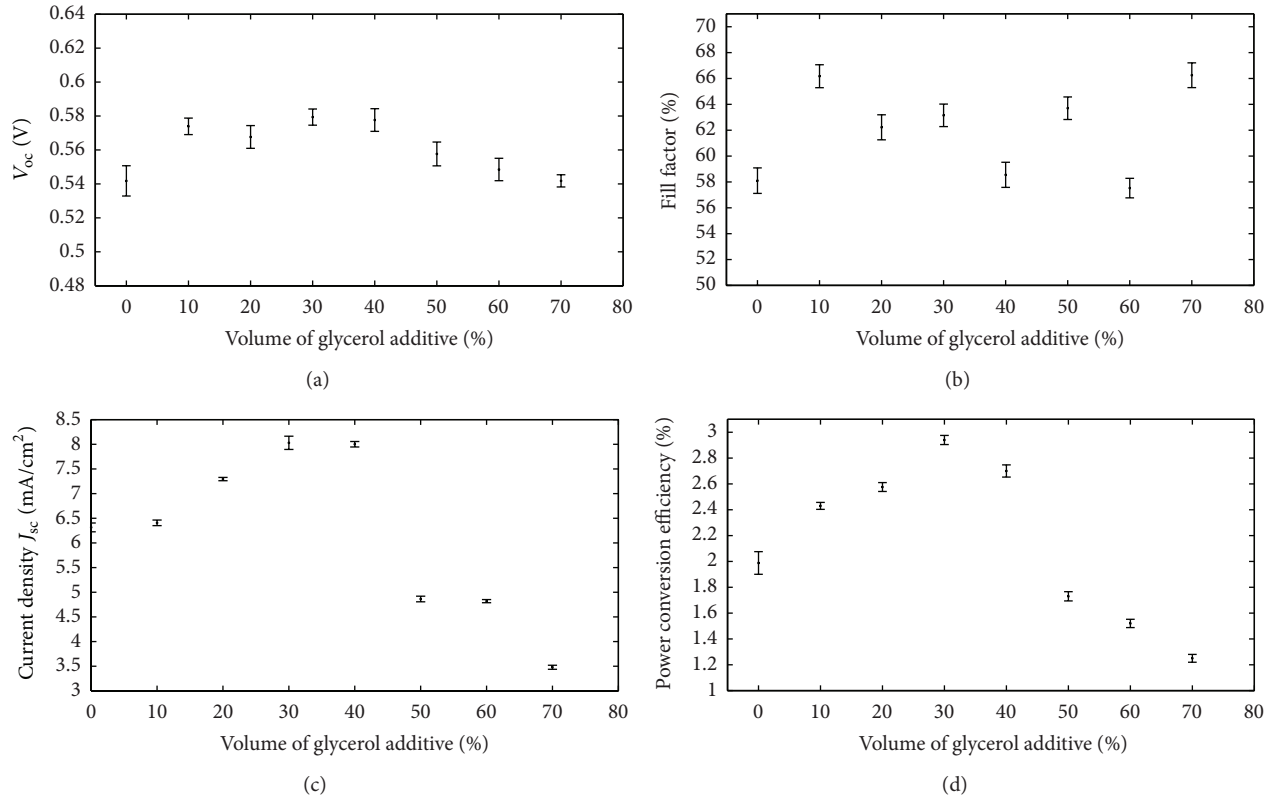

Figure 2: The average variation of photovoltaic parameters with different glycerol concentrations in the active layer.

significantly with 30 vol% glycerol addition, in comparison to pristine devices. Figure 2 shows the average variation of photovoltaic parameters with varying glycerol concentrations.

From Figure 2(a), we can observe that there are gain V_{oc} values from 0 vol% till 30 vol% glycerol additive in the active layer and the value decreases with further increasing concentration of glycerol. From Figure 2(b), although the FF value was the highest for 70 vol% of glycerol additive but significantly generated lower J_{sc} values in Figure 2(c), from Figures 2(a), 2(b), and 2(c), it is clear that, at 30 vol% concentration of glycerol additive, the parameters have higher value for V_{oc} and J_{sc}. The FF was having an appreciable value of 63.15% for 30 vol% glycerol additive compared to other concentrations. The significantly higher V_{oc}, J_{sc}, and good FF values together gave a higher PCE value of almost 3% for 30 vol% glycerol added active layer, which can be observed in Figure 2(d). The reason for enhancement in device performance may be due to the fact that glycerol has a high boiling point which helps in extending the time of the solvent to evaporate thus giving enough time for both P3HT and $PC_{60}BM$ components of the active layer to self-organise and achieve better morphology. Although after the annealing, there can be some residual glycerol present in the active layer owing to the higher boiling point, it can be understood from Figures 1 and 2 that the electrical performance of the layer is enhanced till 30 vol% of glycerol additive.

In the case of a pristine active layer blend, the annealing treatment can cause a rapid evaporation of solvents, thus paving the way to the creation of morphological instability [15]. It has an adverse effect on the blend, especially $PC_{60}BM$. It was reported that, during annealing treatments, $PC_{60}BM$ in the active layer blend can increase in size to unfavourable ranges, normally in micrometers [9, 16]. The most preferred state is the situation when there is nanoscale bicontinuos network between P3HT and $PC_{60}BM$ and there are no excessive crystalisation of components in micrometer scales, thus leading to a better donor-acceptor interface contact area and hence creating a continous path along which carriers can be transported to electrodes [8]. The other reported additive method to enhance performance of P3HT:$PC_{60}BM$ solar cells is the use of 1,2,3,4-tetrahydronaphtahlene (THN) [17] and bisadduct of [6, 6]-phenyl-C61-butyric acid methyl ester (bis-$PC_{60}BM$) [9]. The incorporation of bis-$PC_{60}BM$ in the active layer improved the PCE value by 17%. In the case of THN additive in the active layer, the PCE value was enhanced by only 15%. The 30 vol% of glycerol additive in the active layer enhanced the efficiency by 42% from its initial PCE value. Clearly glycerol additive which is much cheaper and easily processable was enhancing the efficiency of the device to a better extent compared with other reported additives like THN and bis-$PC_{60}BM$.

3.2. Understanding the Effect of Annealing $PC_{60}BM$ Material with and without Glycerol Additive. Since the excessive crystallization of $PC_{60}BM$ occurs in micrometer ranges, it can be observed by an optical microscope.

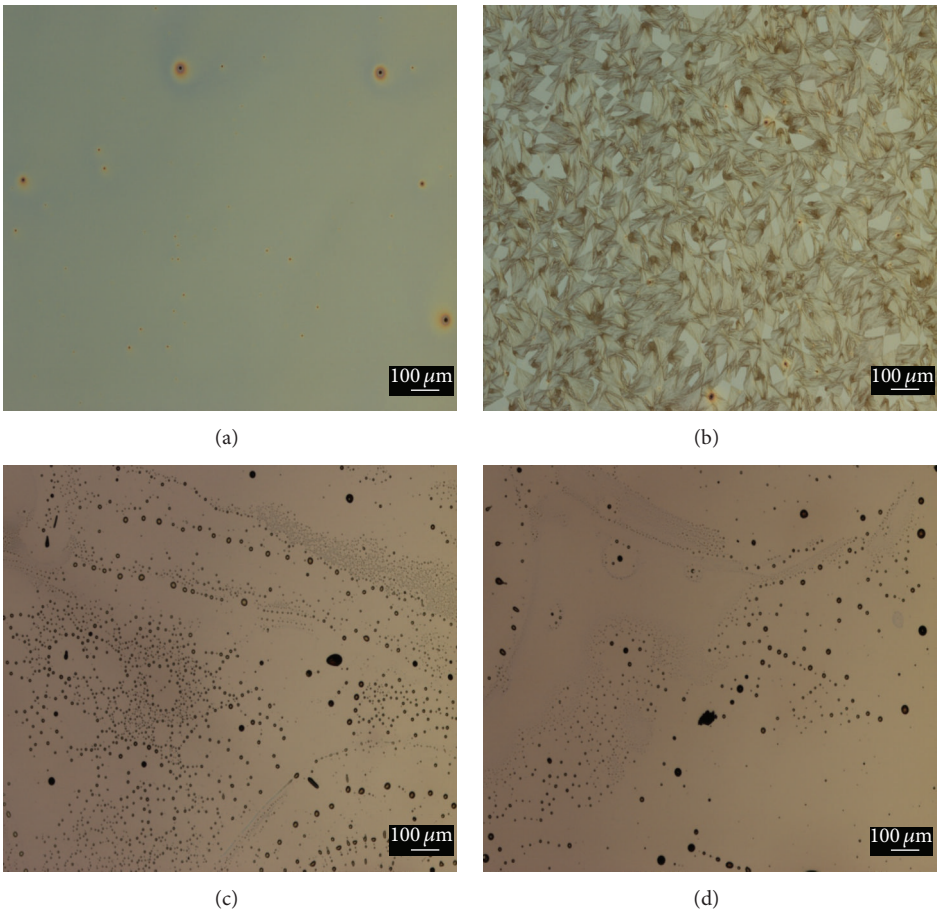

Figure 3: Optical microscope images, scale 100 μm: (a) pristine $PC_{60}BM$ layer unannealed, (b) pristine $PC_{60}BM$ layer annealed, (c) P3HT:$PC_{60}BM$ layer with 30 vol% glycerol additive unannealed, and (d) P3HT:$PC_{60}BM$ layer with 30 vol% glycerol additive annealed.

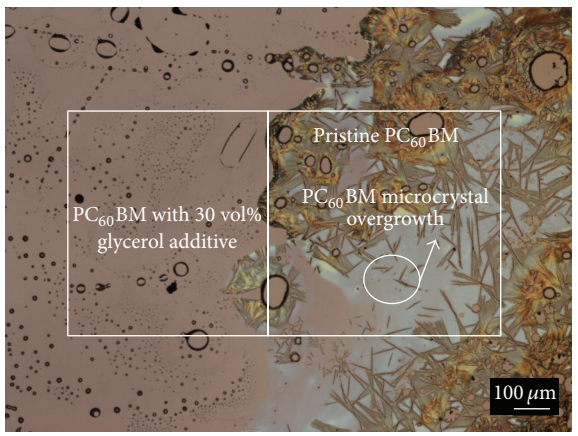

Figure 4: Optical microscope image of the split analysis, scale 100 μm.

In Figure 3(a), the pristine $PC_{60}BM$ which was dissolved in DCB is spin-coated on a glass substrate. Figure 3(b) represents the layer after the annealing treatment. The annealing was done as previously mentioned. The clusters of micrometer range $PC_{60}BM$ components can be seen from Figure 3(b), and this excessive crystallization occured because of the annealing treatment. Figures 3(c) and 3(d) represent the $PC_{60}BM$ blend made in DCB with 30 vol% glycerol additive, before and after annealing treatments, respectively. After the annealing treatment, the large clusters of crystallized components were not observed for the $PC_{60}BM$ blend with the glycerol additive. The excessive crystallization is restricted by

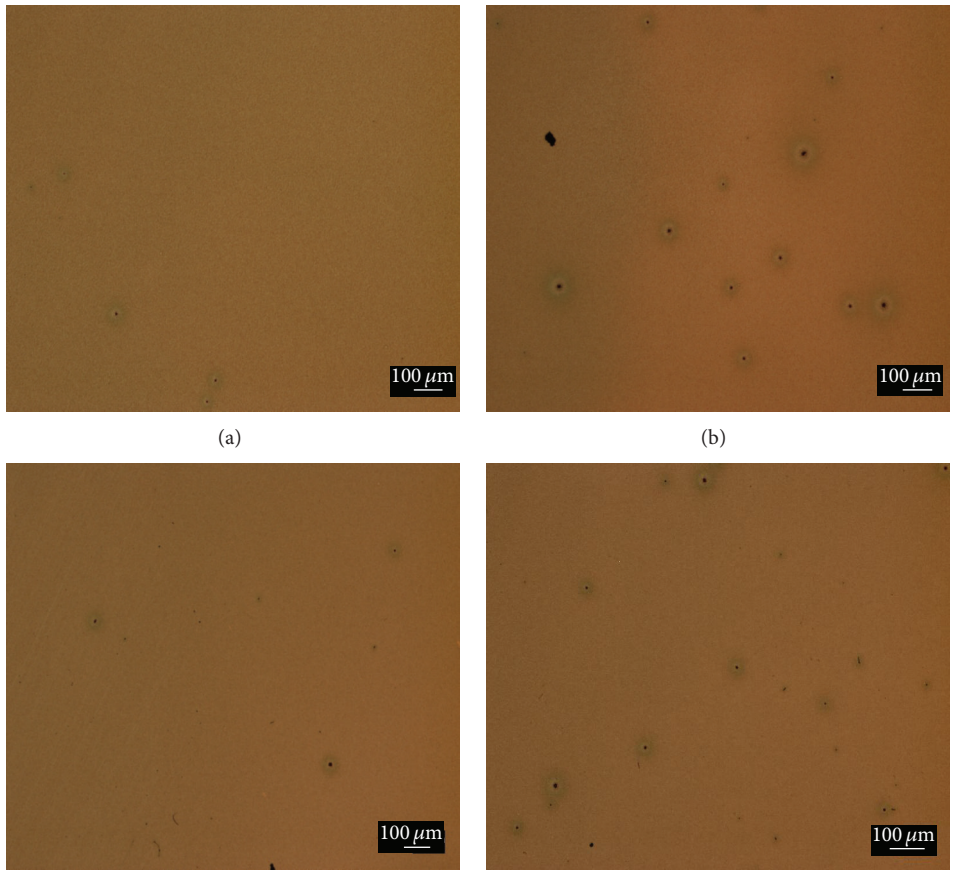

(a) (b) (c) (d)

Figure 5: Optical microscope images; scale is 100 μm: (a) pristine P3HT layer unannealed, (b) pristine P3HT layer annealed, (c) P3HT layer with 30 vol% glycerol additive unannealed, and (d) P3HT layer with 30 vol% glycerol additive annealed.

the presence of glycerol. However, in Figures 3(c) and 3(d), some black spots can be observed by the presence of glycerol. The reason for, and effect of, these was not clearly known within the scope of this study.

In order to better understand the action of glycerol, a split analysis was done. In this analysis, a glass substrate was coated with the pristine $PC_{60}BM$ on one side and the $PC_{60}BM$ blend with the glycerol additive was coated close to it. Then it was annealed in the same way as previously mentioned, and the interface was analysed.

In Figure 4, the area, where the glycerol additive is present, contains no crystallites of a large size. The place that contains the pristine $PC_{60}BM$ blend has a large extent of crystal overgrowth. It is thus evident from this split analysis that the crystal overgrowth is reduced by the presence of the glycerol additive.

3.3. Understanding the Effect of Annealing on P3HT Polymers with and without Glycerol Additive. It is also interesting to see if there are any similar effects of excessive crystallization in P3HT. To understand the effect, the process in Figure 3 was repeated for pristine P3HT and P3HT with the glycerol additive.

Figure 5(a) represents the pristine P3HT blend dissolved in DCB that was spin-coated on a glass substrate and Figure 5(b) represents the layer after the annealing treatment. Figures 5(c) and 5(d) represent blend layers with 30 vol% glycerol, before and after annealing, respectively. In Figures 5(b) and 5(d), large micrometer-sized crystal overgrowth similar to $PC_{60}BM$ is not observed. Thus, it clarifies the fact that the instability in the morphology of P3HT:$PC_{60}BM$ is predominantly from the acceptor material sensitivity towards the heating treatments and the crystal overgrowth is contributed mostly from $PC_{60}BM$.

3.4. Analyzing the Effect of Glycerol Addition in the Active Layer Blend of P3HT:$PC_{60}BM$. Further, it is interesting to analyze what happens in the real active layer blend. It was thus investigated by optical microscope on the structure ITO\PH500\active layer. The active layers were the pristine P3HT:$PC_{60}BM$ blend and a blend with 30 vol% glycerol additive.

Figure 6(a) represents the structure with a pristine active layer, ITO\PH500\P3HT:PC60BM (pristine), while Figure 6(b) represents the layer after annealing. The annealing treatments were done in the same way as previously

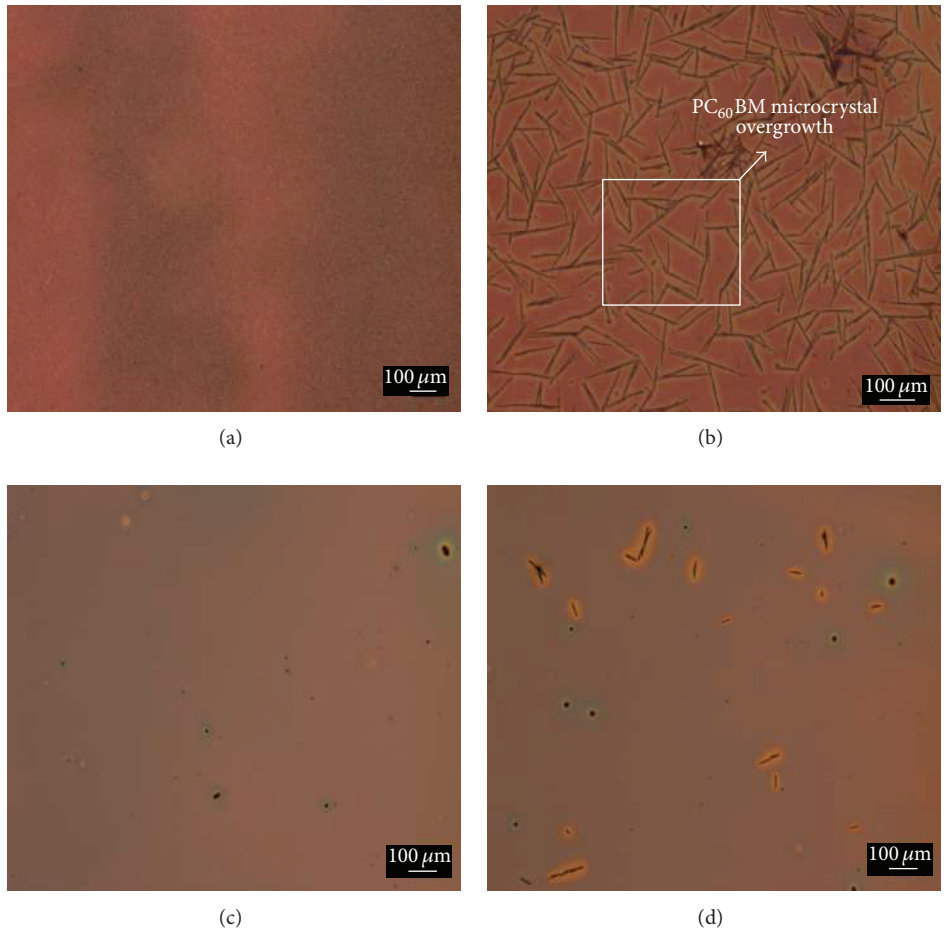

Figure 6: Optical microscope images, scale 100 μm: (a) ITO\PH500\P3HT:PC_{60}BM (pristine) unannealed, (b) ITO\PH500\P3HT:PC_{60}BM (pristine) annealed, (c) ITO\PH500\P3HT:PC_{60}BM layer (with 30 vol% glycerol additive) unannealed, and (d) ITO\PH500\P3HT:PC_{60}BM (with glycerol 30 vol% additive) annealed.

mentioned. Figures 6(c) and 6(d) represent layers with glycerol additive in the active layer, ITO\PH500\P3HT:PC_{60}BM (30 vol% of glycerol additive), before annealing and after annealing, respectively. In Figure 6(b), large PC_{60}BM crystal overgrowth formations can be observed after the annealing treatment. In Figure 6(d), the blend containing the glycerol additive has a reduced number of crystal overgrowth formations. Since glycerol may be providing slow solvent evaporation due to its high boiling point, it can also lead to a smoother film surface and improved vertical phase separation, resulting in efficient percolation pathways and enhanced charge collection [18]. Since glycerol extends the time for the solvent in the active layer to evaporate, it may also provide the P3HT and PC_{60}BM components in the active layer with enough time to self-organize which also reduces rapid crystallization.

To study the changes in roughness with the additive treatment, atomic force microscopy (AFM) was employed.

From the AFM image, Figure 7(a), the root mean square roughness (RMS) for the device structure ITO\PH500\P3HT:PC_{60}BM (pristine) which was not annealed was 15 nm and increased to 16.5 nm after the annealing treatment, Figure 7(b). In the case of the device structure with the glycerol additive in the active layer, that is, ITO\PH500\P3HT:PC_{60}BM (30 vol% of glycerol additive) which was not annealed, Figure 7(c), the RMS value decreased to 7.18 nm and, after annealing, it slightly increased to 7.37 nm. It is thus clear from the AFM measurements that the layer becomes considerably smoother after glycerol addition. It was reported that [16, 19] a smoother surface is likely to improve the adhesion between the electrode and the active layer, thereby reducing recombination of charge carriers at the interface and increasing device efficiency. Since the layer becomes smoother with glycerol addition, it can be understood that the adhesion between the LiF/Al electrodes with the active layer is enhanced and thus also helped in increasing the efficieny. The effects of glycerol, by both restricting the PC_{60}BM crystal overgrowth and smoothening of the active layer, synergetically paved the way to enhance device efficiency. In our future work, the combined effect of glycerol by

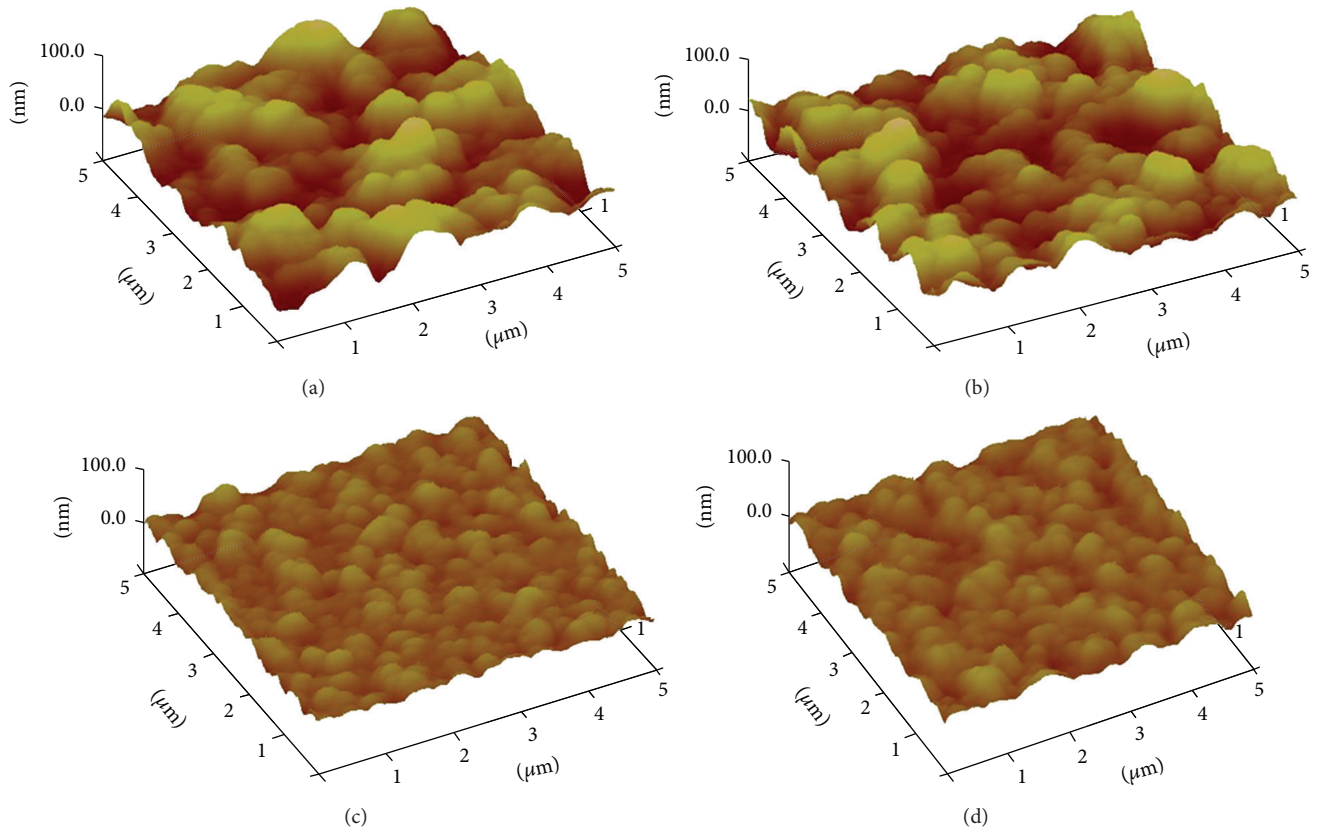

FIGURE 7: AFM height images (a) ITO\PH500\P3HT:PC_{60}BM (pristine) unannealed, RMS roughness 15 nm, (b) ITO\PH500\P3HT:PC_{60}BM (pristine) annealed, RMS roughness 16.5 nm, (c) ITO\PH500\P3HT:PC_{60}BM layer (with 30 vol% glycerol additive) unannealed, RMS roughness 7.18 nm, and (d) ITO\PH500\P3HT:PC_{60}BM (with glycerol 30 vol% additive) annealed, RMS roughness 7.37 nm.

its presence in both the hole transporting layer and the active layer will be explored, with a view on enhancing device efficiency further.

4. Conclusion

In summary, we have enhanced device performance by succesfully restricting the crystal overgrowth of PC_{60}BM by 30 vol% of glycerol additive in the active layer. Moreover, the glycerol addition led to a smoother film surface and also improved electrical properties. The power conversion efficiency was significantly increased from 2.1% to 3%. The glycerol addition technique used is very inexpensive and easily processable.

Conflict of Interests

The authors declare that there is no conflict of interests regarding the publication of this paper.

Acknowledgment

The authors would like to thank the Center for Environment and Energy (CEE) (part of University of Oulu, Finland) for the CEE Innovation Grant for partial funding of our research.

References

[1] A. L. Roes, E. A. Alsema, K. Blok, and M. K. Patel, "Ex-ante environmental and economic evaluation of polymer photovoltaics," *Progress in Photovoltaics: Research and Applications*, vol. 17, no. 6, pp. 372–393, 2009.

[2] C. J. Brabec, N. S. Sariciftci, and J. C. Hummelen, "Plastic solar cells," *Advanced Functional Materials*, vol. 11, pp. 15–26, 2001.

[3] R. Po, C. Carbonera, A. Bernardi, F. Tinti, and N. Camaioni, "Polymer- and carbon-based electrodes for polymer solar cells: toward low-cost, continuous fabrication over large area," *Solar Energy Materials and Solar Cells*, vol. 100, pp. 97–114, 2012.

[4] B. Augustine, R. Sliz, K. Lahtonen, M. Valden, R. Myllylä, and T. Fabritius, "Effect of plasma treated Ag/indium tin oxide anode modification on stability of polymer solar cells," *Solar Energy Materials and Solar Cells*, vol. 128, pp. 330–334, 2014.

[5] W. Cao and J. Xue, "Recent progress in organic photovoltaics: device architecture and optical design," *Energy & Environmental Science*, vol. 7, no. 7, pp. 2123–2144, 2014.

[6] H. Hoppe and N. S. Sariciftci, "Morphology of polymer/fullerene bulk heterojunction solar cells," *Journal of Materials Chemistry*, vol. 16, no. 1, pp. 45–61, 2006.

[7] J. J. M. Halls, A. C. Arias, J. D. MacKenzie et al., "Photodiodes based on polyfluorene composites: influence of morphology," *Advanced Materials*, vol. 12, no. 7, pp. 498–502, 2000.

[8] C. Müller, T. A. M. Ferenczi, M. Campoy-Quiles et al., "Binary organic photovoltaic blends: a simple rationale for optimum

compositions," *Advanced Materials*, vol. 20, no. 18, pp. 3510–3515, 2008.

[9] H. W. Liu, D. Y. Chang, W. Y. Chiu, S. P. Rwei, and L. Wang, "Fullerene bisadduct as an effective phase-separation inhibitor in preparing poly(3-hexylthiophene)-[6,6]-phenyl-C 61-butyric acid methyl ester blends with highly stable morphology," *Journal of Materials Chemistry*, vol. 22, no. 31, pp. 15586–15591, 2012.

[10] A. J. Moulé and K. Meerholz, "Controlling morphology in polymer-fullerene mixtures," *Advanced Materials*, vol. 20, no. 2, pp. 240–245, 2008.

[11] S. Bertho, G. Janssen, T. J. Cleij et al., "Effect of temperature on the morphological and photovoltaic stability of bulk heterojunction polymer:fullerene solar cells," *Solar Energy Materials and Solar Cells*, vol. 92, no. 7, pp. 753–760, 2008.

[12] S. Miyanishi, K. Tajima, and K. Hashimoto, "Morphological stabilization of polymer photovoltaic cells by using cross-linkable poly(3-(5-hexenyl)thiophene)," *Macromolecules*, vol. 42, no. 5, pp. 1610–1618, 2009.

[13] D. R. Lide, Ed., *CRC Handbook of Data on Organic Compounds*, CRC Press, Boca Raton, Fla, USA, 3rd edition, 1994.

[14] W. Ma, C. Yang, X. Gong, K. H. Lee, and A. J. Heeger, "Thermally stable, efficient polymer solar cells with nanoscale control of the interpenetrating network morphology," *Advanced Functional Materials*, vol. 15, no. 10, pp. 1617–1622, 2005.

[15] K. E. Strawhecker, S. K. Kumar, J. F. Douglas, and A. Karim, "The critical role of solvent evaporation on the roughness of spin-cast polymer films," *Macromolecules*, vol. 34, no. 14, pp. 4669–4672, 2001.

[16] P. Dutta, Y. Xie, M. Kumar et al., "Connecting physical properties of spin-casting solvents with morphology, nanoscale charge transport, and device performance of poly(3-hexylthiophene): phenyl-C61-butyric acid methyl ester bulk heterojunction solar cells," *Journal of Photonics for Energy*, vol. 1, no. 1, Article ID 011124, 2011.

[17] A. De Sio, T. Madena, R. Huber et al., "Solvent additives for tuning the photovoltaic properties of polymerfullerene solar cells," *Solar Energy Materials and Solar Cells*, vol. 95, no. 12, pp. 3536–3542, 2011.

[18] A. C. Arias, "Vertically segregated polymer blends: their use in organic electronics," *Journal of Macromolecular Science Part C: Polymer Reviews*, vol. 46, no. 1, pp. 103–125, 2006.

[19] S. E. Shaheen, C. J. Brabec, N. S. Sariciftci, F. Padinger, T. Fromherz, and J. C. Hummelen, "2.5% efficient organic plastic solar cells," *Applied Physics Letters*, vol. 78, no. 6, pp. 841–843, 2001.